

RESEARCH ARTICLE

Augmented *Pla2g4c/Ptgs2/Hpgds* axis in bronchial smooth muscle tissues of experimental asthma

Yoshihiko Chiba^{1*}, Wataru Suto¹, Hiroyasu Sakai²

1 Department of Physiology and Molecular Sciences, School of Pharmacy, Hoshi University, Tokyo, Japan, **2** Department of Analytical Pathophysiology, School of Pharmacy, Hoshi University, Tokyo, Japan

* chiba@hoshi.ac.jp



Abstract

Rationale

Augmented smooth muscle contractility of the airways is one of the causes of airway hyper-responsiveness in asthmatics. However, the mechanism of the altered properties of airway smooth muscle cells is not well understood.

Objectives

To identify differentially expressed genes (DEGs) related to the bronchial smooth muscle (BSM) hyper-contraction in a murine asthma model.

Methods

The ovalbumin (OA)-sensitized mice were repeatedly challenged with aerosolized OA to induce asthmatic reaction. Transcriptomic profiles were generated by microarray analysis of BSM tissues from the OA-challenged and control animals, and KEGG (Kyoto Encyclopedia of Genes and Genomes) Pathway Analysis was applied.

Measurements and main results

Tension study showed a BSM hyperresponsiveness to acetylcholine (ACh) in the OA-challenged mice. A total of 770 genes were differentially expressed between the OA-challenged and control animals. Pathway analysis showed a significant change in arachidonic acid (AA) metabolism pathway in BSM tissues of the OA-challenged mice. Validation of DEGs by quantitative RT-PCR showed a significant increase in PLA₂ group 4c (*Pla2g4c*)/COX-2 (*Ptgs2*)/PGD₂ synthase 2 (*Hpgds*) axis. PGD₂ level in bronchoalveolar fluids of the OA-challenged mice was significantly increased. A 24-h incubation of BSM tissues with PGD₂ caused a hyperresponsiveness to ACh in naive control mice.

Conclusions

AA metabolism is shifted towards PGD₂ production in BSM tissues of asthma. Increased PGD₂ level in the airways might be a cause of the BSM hyperresponsiveness in asthma.

OPEN ACCESS

Citation: Chiba Y, Suto W, Sakai H (2018) Augmented *Pla2g4c/Ptgs2/Hpgds* axis in bronchial smooth muscle tissues of experimental asthma. PLoS ONE 13(8): e0202623. <https://doi.org/10.1371/journal.pone.0202623>

Editor: Brian J. Knoll, University of Houston, UNITED STATES

Received: May 26, 2018

Accepted: August 7, 2018

Published: August 30, 2018

Copyright: © 2018 Chiba et al. This is an open access article distributed under the terms of the [Creative Commons Attribution License](https://creativecommons.org/licenses/by/4.0/), which permits unrestricted use, distribution, and reproduction in any medium, provided the original author and source are credited.

Data Availability Statement: All microarray files are available from the Gene Expression Omnibus (GEO) database (accession number GSE116504).

Funding: This work was partly supported by Grant-in-Aid for Scientific Research (C) Grant Number 15K08248 (YC) from the Japan Society for the Promotion of Science (JSPS). The funders had no role in study design, data collection and analysis, decision to publish, or preparation of the manuscript.

Competing interests: The authors have declared that no competing interests exist.

Abbreviations: 12-HHT, 12S-hydroxy-5Z,8E,10E-heptadecatrienoic acid; 15-HETE, 15-hydroxy-5Z,8Z,11Z,13E-eicosatetraenoic acid; AA, arachidonic acid; ACh, acetylcholine; ACT, actin; AHR, airway hyperresponsiveness; ANOVA, analysis of variance; BAL, bronchoalveolar lavage; BSM, bronchial smooth muscle; CALD, caldesmon; COX, cyclooxygenase; cRNA, complementary RNA; C_T, threshold cycle; dCTP, deoxycytidine triphosphate; DEG, differentially expressed gene; FDR, false discovery rate; GO, gene ontology; HPGDS, prostaglandin D₂ synthase 2 (hematopoietic PGD synthase); KEGG, Kyoto Encyclopedia of Genes and Genomes; LC/MS/MS, liquid chromatography/tandem mass spectrometry; LPE, local pooled error; LT, leukotriene; miRNA, microRNA; MYH, myosin heavy chain; MYL, myosin light chain; MYLK, myosin light chain kinase; OA, ovalbumin; PG, prostaglandin; PLA₂, phospholipase A₂; PLA2G4C, phospholipase A₂ group 4c; PLB1, phospholipase B₁; PPP1, protein phosphatase 1; PTGIS, prostaglandin I₂ synthase; PTGS2, prostaglandin-endoperoxide synthase 2 (cyclooxygenase-2); TBXAS1, thromboxane A synthase; TNF, tumor necrosis factor.

Introduction

Enhanced airway responsiveness to non-specific stimuli, called airway hyperresponsiveness (AHR), is a characteristic feature of bronchial asthma. One of the causes of the AHR is hyper-contraction of smooth muscle cells of the airways [1–5]. Rapid relief from airway limitation in asthma attack by short-acting beta₂-stimulant inhalation may also suggest an involvement of augmented airway smooth muscle contraction in the airway obstruction. It is thus important for development of asthma therapy to understand the disease-related changes in the contractile signaling of airway smooth muscle cells.

Smooth muscle contraction is caused by the interaction of myosin and actin filaments, and regulated by various contractile and Ca²⁺-sensitizing proteins [6, 7]. One possible explanation of the hyper-contraction of smooth muscle may be an up-regulation of these proteins associated with contraction. In addition to their contractile function, smooth muscle cells of the airways also have ability to generate/secrete various biologically active substances including interleukins, chemokines, and prostanoids [8–13]. The airway structural cells, such as epithelial cells (*e.g.*, [14]), and the accumulated inflammatory cells, such as eosinophils (*e.g.*, [15]), also release various mediators around the smooth muscle cells. Some of these autocrine/paracrine mediators affect transcriptional signaling in the cells of airway smooth muscle, resulting in an alteration of its function [12, 16–19]. Thus, an inclusive analysis of differentially expressed genes in airway smooth muscle tissues of asthma might provide new insight into the treatment of the AHR.

In the present study, we used a well-characterized asthma model of mice, which have AHR both *in vivo* and *in vitro* [20]. A microarray analysis was applied to identify the differentially expressed genes in BSM tissues of the AHR animals. Gene Ontology (GO) and Kyoto Encyclopedia of Genes and Genomes (KEGG) pathway analyses revealed the arachidonic acid metabolism pathway as a significantly changed pathway associated with AHR. In particular, an augmentation of phospholipase A₂ group 4c (*Pla2g4c*)/cyclooxygenase-2 (*Ptgs2*)/prostaglandin D₂ synthase 2 (*Hpgds*) cascade was strongly suggested. Thus, the role of prostaglandin D₂ (PGD₂) in the development of BSM hyperresponsiveness, one of the causes of AHR, was also investigated.

Materials and methods

Animals and treatments

Male BALB/c mice were purchased from the Tokyo Laboratory Animals Science Co., Ltd. (Tokyo, Japan) and housed in a pathogen-free facility. All animal experiments were approved by the Animal Care Committee of the Hoshi University (Tokyo, Japan).

Preparation of a murine model of allergic bronchial asthma, which has an *in vivo* AHR [20], was performed as described previously [18, 21]. In brief, BALB/c mice (8 weeks of age) were actively sensitized by intraperitoneal injections of 8 μg ovalbumin (OA; Seikagaku Co., Tokyo, Japan) with 2 mg Imject Alum (Pierce Biotechnology, Inc., Rockford, IL, USA) on Day 0 and Day 5. The sensitized mice were challenged with aerosolized OA-saline solution (5 mg/mL) for 30 min on Days 12, 16 and 20. A control group of mice received the same immunization procedure but inhaled saline aerosol instead of OA challenge. The aerosol was generated with a compressor nebulizer (MiniElite™: Philips Respironics, NV, USA) and introduced to a Plexiglas chamber box (130 x 200 mm, 100 mm height) in which the mice were placed. Twenty-four h after the last OA challenge, mice were sacrificed by exsanguination from abdominal aorta under urethane (1.6 g/kg, *i.p.*; Sigma, St. Louis, MO) anesthesia.

RNA extraction

Both left and right main bronchi were isolated, and the epithelia, capillary vessels and connective tissues were removed as much as possible (S1 Fig) by gently rubbing with sharp tweezers under a stereomicroscope [21]. Total RNA was extracted using Trizol reagent (Invitrogen, Karlsruhe, Germany) according to the manufacturer's protocol. RNA purity and integrity were evaluated by ND-1000 Spectrophotometer (Thermo Fisher Scientific, Waltham, MA) and Agilent 2100 Bioanalyzer (Agilent Technologies, Santa Clara, CA).

Microarray analysis

RNA labeling and hybridization were performed by using the Agilent One-Color Microarray-Based Gene Expression Analysis protocol (v6.5, Agilent Technologies). Briefly, total RNA (100 ng) of each sample was linearly amplified and labeled with Cy3-dCTP. The labeled cRNAs were purified using RNeasy Mini Kit (Qiagen, Valencia, CA). The concentration and specific activity of the labeled cRNAs (pmol Cy3/ μ g cRNA) were measured by NanoDrop ND-1000 (Thermo Fisher Scientific Inc.). Each labeled cRNA (600 ng) was fragmented by adding 5 μ L 10 x blocking agent and 1 μ L of 25 x fragmentation buffer, and then heated at 60°C for 30 min. Finally 25 μ L 2 x GE hybridization buffer was added to dilute the labeled cRNA. The hybridization solution (40 μ L) was dispensed into the gasket slide and assembled to the Agilent SurePrint G3 Mouse GE 8X60K, v2 Microarrays (Agilent Technologies). The slides were incubated for 17 h at 65°C in an Agilent hybridization oven, and then washed at room temperature by using the Agilent One-Color Microarray-Based Gene Expression Analysis protocol (v6.5, Agilent Technologies). The hybridized array was immediately scanned with an Agilent Microarray Scanner D (Agilent Technologies).

The captured array images were analyzed using Agilent Feature Extraction Software (v11.0.1.1, Agilent Technologies). The raw data for same gene was then summarized automatically in Agilent Feature Extraction Protocol to generate raw data text file, providing expression data for each gene probed on the array. Array probes that have Flag A in samples were filtered out. Selected gProcessedSignal value was transformed by logarithm and normalized by quantile method. Statistical significance of the expression data was determined using fold change and local pooled error (LPE) test in which the null hypothesis was that no difference exists between the groups. Hierarchical cluster analysis was performed using complete linkage and Euclidean distance as a measure of similarity. Gene Ontology (GO) functional enrichment analysis for the differentially expressed genes was performed using Gene Set Enrichment Analysis software (<http://software.broadinstitute.org/gsea/index.jsp>). The gene sets were separated according to the GO terms for biological processes, cellular components, and molecular functions. Pathway analysis was performed using GeneCodis tools (<http://genecodis.cnb.csic.es>) based on the Kyoto Encyclopedia of Genes and Genomes (KEGG: <https://www.kegg.jp>) pathway database. All data analysis and visualization of differentially expressed genes was conducted using R 3.0.2 (www.r-project.org).

Quantitative RT-PCR analyses

Expression levels of mRNA transcripts were determined by quantitative RT-PCR analysis. In brief, reverse transcription reactions were performed using a cDNA synthesis kit (RR037A: TaKaRa, Shiga, Japan) according to the manufacturer's instructions. The cDNA products from each sample were then subjected to real-time PCR analyses using StepOne™ real-time PCR system (Applied Biosystems, Foster City, CA) with Fast SYBR Green Master Mix (Applied Biosystems) according to the manufacturer's instructions. The reactions were incubated in a 48-well optical plate at 95°C for 20 seconds, following by 43 cycles of 95°C for 3 seconds and 60°C for

Table 1. Primer sequences for RT-PCR used in the present study.

| Gene name | RefSeq Accession | | Sequence | Amplicon size |
|---------------|-------------------------|-----------|---------------------------------|---------------|
| mouse Pla2g4c | NM_001168504 | Sense | 5' -GGACCGTTGCGTTTTTGTGA-3' | 150 bp |
| | | Antisense | 5' -GC AAA ACCAGCATCCACCAG-3' | |
| mouse Cyp4f18 | NM_024444 | Sense | 5' -CTTCAGGGATGCATGCTGCT-3' | 124 bp |
| | | Antisense | 5' -GAAGACTGTGTCCTTGGGGG-3' | |
| mouse Alox12e | NM_145684 | Sense | 5' -CTGAGGTTGGACTGCTTGGA-3' | 124 bp |
| | | Antisense | 5' -TGTGTAGATGCGTGCTGACC-3' | |
| mouse Ptgs2 | NM_011198 | Sense | 5' -CCGTGGGGAATGTATGAGCA-3' | 128 bp |
| | | Antisense | 5' -GGTGGGCTTCAGCAGTAAT-3' | |
| mouse Hpgds | NM_019455 | Sense | 5' -TTCCATGGGCAGAGAAAGA-3' | 143 bp |
| | | Antisense | 5' -GCCAGGTTACATAATGCCT-3' | |
| mouse Cyp2e1 | NM_021282 | Sense | 5' -CGAGGGGACATTCTGTGTT-3' | 140 bp |
| | | Antisense | 5' -CGGGCCTCATTACCTGTTT-3' | |
| mouse Cyp4a10 | NM_010011 | Sense | 5' -ACCTCCACAGGCAATGGCTA-3' | 150 bp |
| | | Antisense | 5' -ATCTAGGAAAGGCACTTGGGAAG-3' | |
| mouse Cyp4a12 | NM_172306, NM_177406 | Sense | 5' -CCTTACACGGAAATCATGGCAG-3' | 112 bp |
| | | Antisense | 5' -AGGTCATCAAGGTGATGTGTTGGA-3' | |
| mouse Gapdh | NM_008084 | Sense | 5' -CCTCGTCCCCTAGACAAAATG-3' | 100 bp |
| | | Antisense | 5' -TCTCCACTTTGCCACTGCAA-3' | |

<https://doi.org/10.1371/journal.pone.0202623.t001>

30 seconds. The PCR primer sets used are shown in Table 1, which were designed from published sequences.

Western blot analyses

Protein samples of the BSM tissues were subjected to 15% sodium dodecyl sulfate-polyacrylamide gel electrophoresis (SDS-PAGE) and the proteins were then electrophoretically transferred to a polyvinylidene fluoride (PVDF) membrane. After blocking with EzBlock Chemi (Atto, Co., Tokyo, Japan), the PVDF membrane was incubated with the primary antibody. The primary antibodies used in the present study were polyclonal rabbit anti-hematopoietic prostaglandin D synthase antibody (HPGDS; 1:200 dilution; Item No. 160013; Cayman Chemical; Ann Arbor, MI). Then the membrane was incubated with horseradish peroxidase-conjugated donkey anti-rabbit IgG (1:2,500 dilution; Santa Cruz Biotechnology, Inc.; Santa Cruz, CA), detected using EzWestBlue (Atto, Co.) and analyzed by a densitometry system. Detection of house-keeping gene was also performed on the same membrane by using monoclonal mouse anti-GAPDH (1:10,000 dilution; Santa Cruz Biotechnology, Inc.).

Assessment of prostaglandin D₂ (PGD₂) levels in BAL fluids

After the exsanguinations, the chest of each animal was opened and a 20-gauge blunt needle was tied into the proximal trachea. Bronchoalveolar lavage (BAL) fluid was obtained by intratracheal instillation of 1 mL/animal of phosphate-buffered saline (PBS; pH 7.5, room temperature) into the lung while it was kept located within the thoracic cavity. The lavage was reinfused into the lung twice before final collection. The BAL fluids were centrifuged at 500 g, and the resultant supernatants were stored at -80°C until use. The levels of PGD₂ in BAL fluids were measured by a competitive PGD₂ ELISA system (Item No. 512011; Cayman Chemical, Ann Arbor, MI) according to the manufacturer's instructions.

Lipidomic profiling by LC mass spectrometry

Lipid mediators were analyzed by LC and MS essentially as described previously [22, 23]. Briefly, BAL fluids were supplemented with a mix consisting of four deuterated internal standards (Cayman Chemical) and lipid metabolites isolated by solid phase extraction on an Oasis HLB column (Waters, Milford, MA). The extracted samples were evaporated, reconstituted in a small volume, and the eicosanoids were separated by reverse phase LC using an XBridge C18 column (Waters). The eicosanoids were analyzed by a triple quadrupole mass spectrometer (LCMS8040, Shimadzu, Kyoto, Japan) operated in the negative-ionization mode via multiple-reaction monitoring (MRM) using transitions that were optimized for selectivity and sensitivity. Quantitation was performed using calibration curves constructed for each compound, and recoveries were monitored using deuterated internal standards (15-HETE-d8, LTB₄-d4, PGE₂-d4, arachidonic acid-d8). Data analysis was performed using LabSolutions software (Shimadzu).

Determination of bronchial smooth muscle (BSM) responsiveness

Mice were sacrificed by exsanguination from abdominal aorta under urethane (1.6 g/kg, *i.p.*) anesthesia and the airway tissues under the larynx to lungs were immediately removed. About 3 mm length of the left main bronchus (about 0.5 mm diameter) was isolated. The resultant tissue ring preparation was then suspended in a 5 mL-organ bath by two stainless-steel wires (0.2 mm diameter) passed through the lumen. For all tissues, one end was fixed to the bottom of the organ bath while the other was connected to a force-displacement transducer (TB-612T, Nihon Kohden) for the measurement of isometric force. A resting tension of 0.5 g was applied. The buffer solution contained modified Krebs-Henseleit solution with the following composition (mM): NaCl 118.0, KCl 4.7, CaCl₂ 2.5, MgSO₄ 1.2, NaHCO₃ 25.0, KH₂PO₄ 1.2 and glucose 10.0. The buffer solution was maintained at 37°C and oxygenated with 95% O₂-5% CO₂. After the equilibration period, the tension studies were performed. In case of the high K⁺ depolarization studies, experiments were conducted in the presence of atropine (10⁻⁶ M).

Data and statistical analyses

In the real-time PCR analyses, the comparative threshold cycle (C_T) method was used for relative quantification of the mRNA transcripts. Differences in the C_T values (ΔC_T) between the target gene and GAPDH were calculated to determine the relative expression levels, using the following formula: ΔΔC_T = (ΔC_T of the treated sample) - (ΔC_T of the control sample). The relative expression level between the samples was calculated according to the equation 2^{-ΔΔC_T}.

All the data were expressed as the mean with S.E. Statistical significance of difference was determined by unpaired Student's *t*-test or two-way analysis of variance (ANOVA) with *post hoc* Bonferroni/Dunn (StatView for Macintosh ver. 5.0, SAS Institute, Inc., NC). A value of *P* < 0.05 was considered significant.

Results

Identification of differentially expressed genes in BSM tissues of the antigen-challenged mice

As shown in Fig 1, the contractile responsiveness to acetylcholine (ACh) was significantly augmented in bronchial smooth muscle (BSM) tissues isolated from the repeatedly antigen-challenged mice. In the present study, total RNA was isolated from BSM tissues of the diseased animals and was used for a DNA microarray analysis.

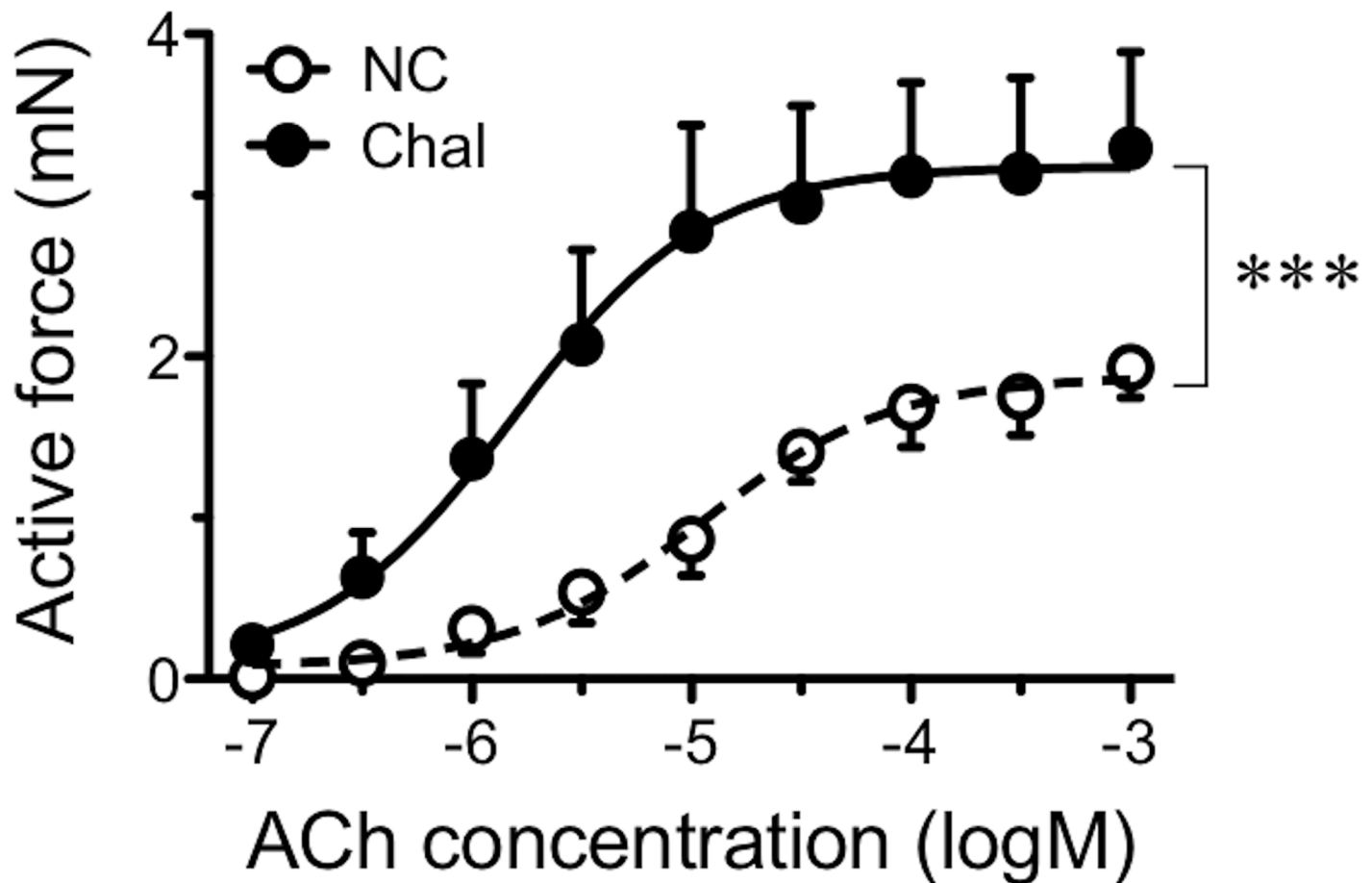


Fig 1. Change in the contractile responsiveness to acetylcholine (ACh) in bronchial smooth muscle tissues of a murine asthma model used in the present study. Male BALB/c mice were actively sensitized and repeatedly challenged with ovalbumin (OA) antigen. Twenty-four hours after the last OA challenge, the left main bronchi were isolated and the ACh responsiveness was measured as described in METHODS. Each point represents the mean \pm SEM from 6 animals, respectively. NC: naive control, and Chal: repeatedly antigen-challenged groups. A significant difference was observed between the groups ($P < 0.001$ by two-way ANOVA with *post hoc* Bonferroni/Dunn test).

<https://doi.org/10.1371/journal.pone.0202623.g001>

As shown in Fig 2A, box-whisker plotting showed similar distribution of intensities among the samples used, suggesting that the array experiment was performed under an appropriate condition. Variations of gene expression among the specimens were shown by volcano plotting (Fig 2B) and scatter plotting (Fig 2C). Of the 56,605 probe sets represented on the Agilent SurePrint G3 Mouse GE 8X60K v2 gene chip, 770 probe sets were differentially expressed in BSM tissues of the antigen-challenged mice as compared with those of control animals ($|\text{fold change}| \geq 2$ and adjusted P -value < 0.05 ; $N = 4$, respectively). Among them, 557 were up-regulated and 213 were down-regulated. An unsupervised hierarchical clustering analysis of the differentially expressed genes showed a distinct separation between the antigen-challenged (C) and normal control animals (N) (Fig 3). The complete data set is publicly available in the Gene Expression Omnibus (GEO) public repository (<http://www.ncbi.nlm.nih.gov/geo/>) (Accession No. GSE116504) in a format that complies with the Minimal Information About a Microarray Experiment guidelines.

Gene ontology analysis and KEGG pathway enrichment analysis

Gene ontology analysis of the differentially expressed genes identified a number of different processes with statistical significance. Fig 4 shows the top 15 gene ontology terms of

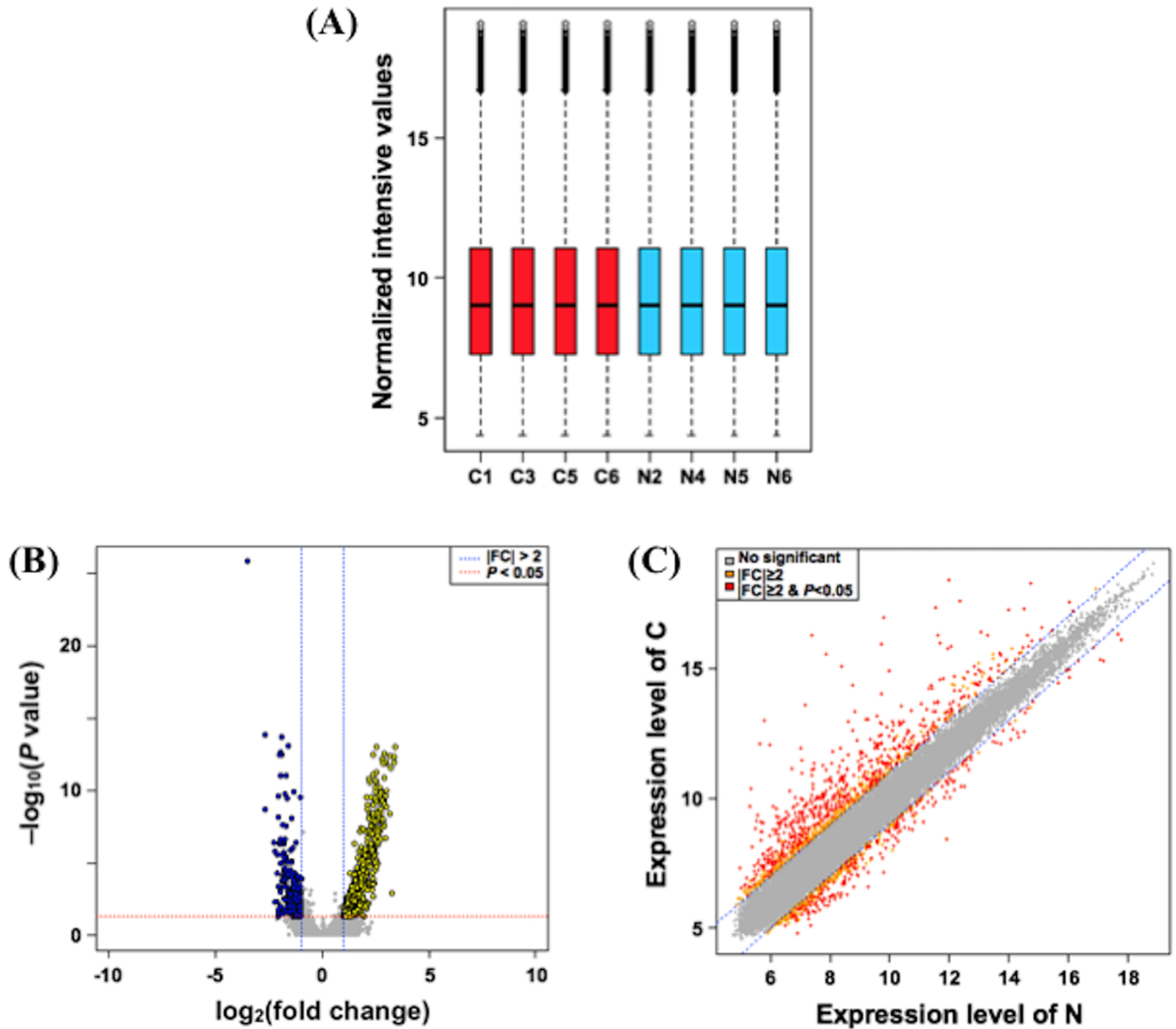


Fig 2. Expression profiles of genes in bronchial smooth muscle tissues of the repeatedly antigen-challenged (C) and normal control (N) mice. Total RNA sample of each mouse (4 animals, respectively) was subjected to the microarray analysis as described in METHODS. (A) Box-whisker plots of genes show the distribution of intensities from all samples. (B) Volcano plots show variation in gene expression. The vertical lines correspond to 2.0-fold up- and down-regulations. The horizontal line represents a P -value of 0.05. (C) Scatter plots show variation in gene expression. FC: fold change.

<https://doi.org/10.1371/journal.pone.0202623.g002>

biological processes (Fig 4A), cellular components (Fig 4B), and molecular function (Fig 4C). The KEGG pathway analysis suggested that 69 pathways were significantly correlated with the differentially expressed genes (adjusted P -value < 0.05 by FDR). These included pathways reported to be associated with asthma, such as Cytokine-cytokine receptor interaction (Map ID: mmu04060: adjusted P -value = $5.5E-11$), Chemokine signaling pathway (Map ID: mmu04062: adjusted P -value = $1.0E-8$), TNF signaling pathway (Map ID: mmu04668: adjusted P -value = $1.9E-6$), and Asthma (Map ID: mmu05310: adjusted P -value = 0.040).

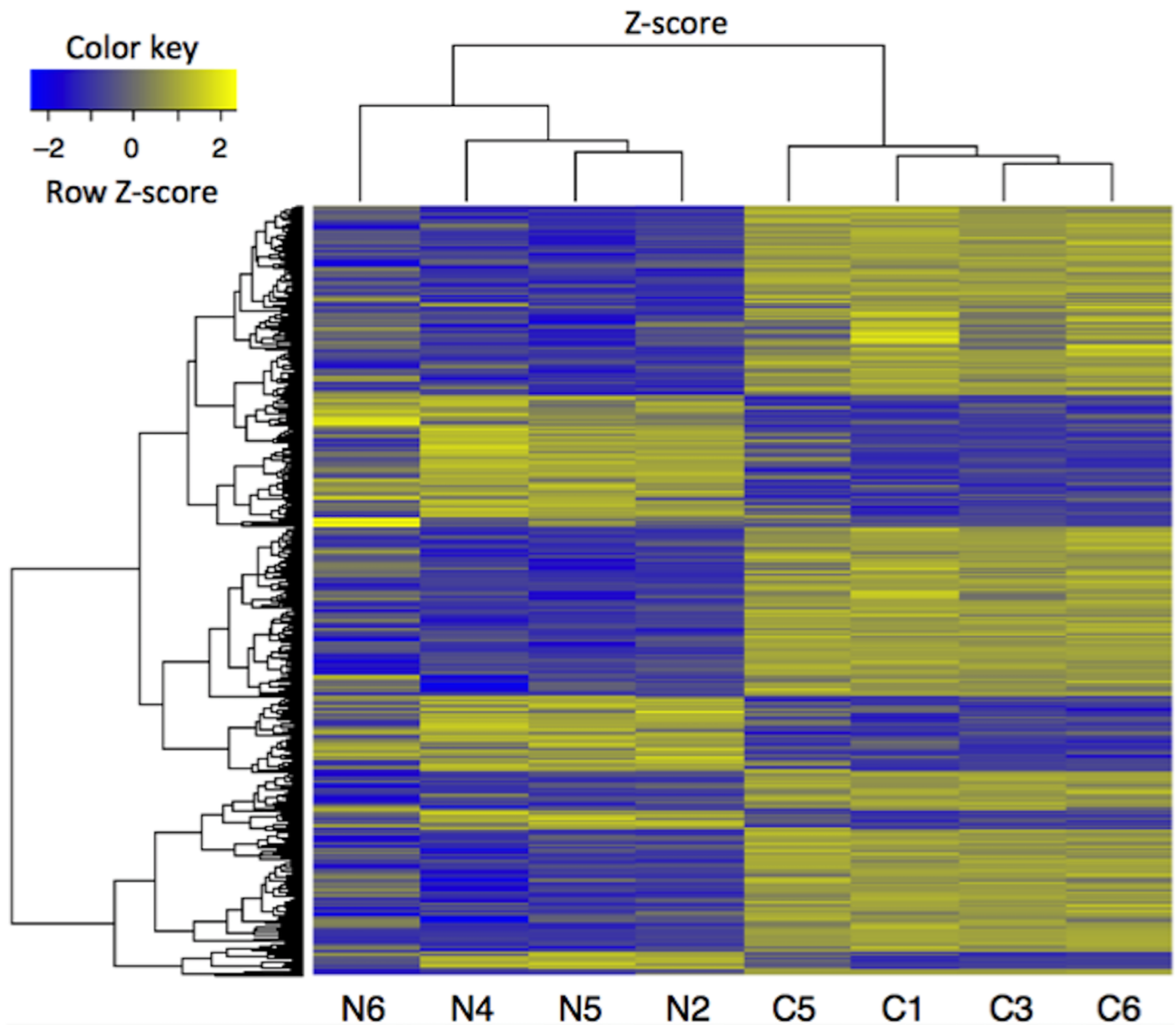


Fig 3. Hierarchical cluster analysis of differentially expressed genes ($|\text{fold change}| \geq 2$ and adjusted P -value < 0.05) in bronchial smooth muscle tissues of the antigen-challenged mice. Total RNA sample of each mouse (4 animals, respectively) was subjected to the microarray analysis, and hierarchical cluster analysis of differentially expressed genes was performed. Each row represents a differentially expressed gene and each column represents an individual mouse. N and C represent the normal control and the repeatedly antigen-challenged groups, respectively. Each group contains four different animals. Colors represent fold change in each individual, with yellow indicating up-regulated genes and blue indicating down-regulated genes with respect to the average of the normal control animals.

<https://doi.org/10.1371/journal.pone.0202623.g003>

When the Bonferroni correction was applied to the data, 32 pathways were suggested as highly significant pathways (adjusted P -value < 0.05 by Bonferroni; Fig 5). Among them, we focused on Arachidonic acid (AA) metabolism pathway (Map ID: mmu00590, Fig 6) in the present study. The AA metabolism pathway comprised 9 differentially expressed genes: 5 of them were significantly up-regulated and 4 of them were significantly down-regulated in BSM tissues of the antigen-challenged mice (adjusted P -value < 0.05 by Bonferroni, Table 2).

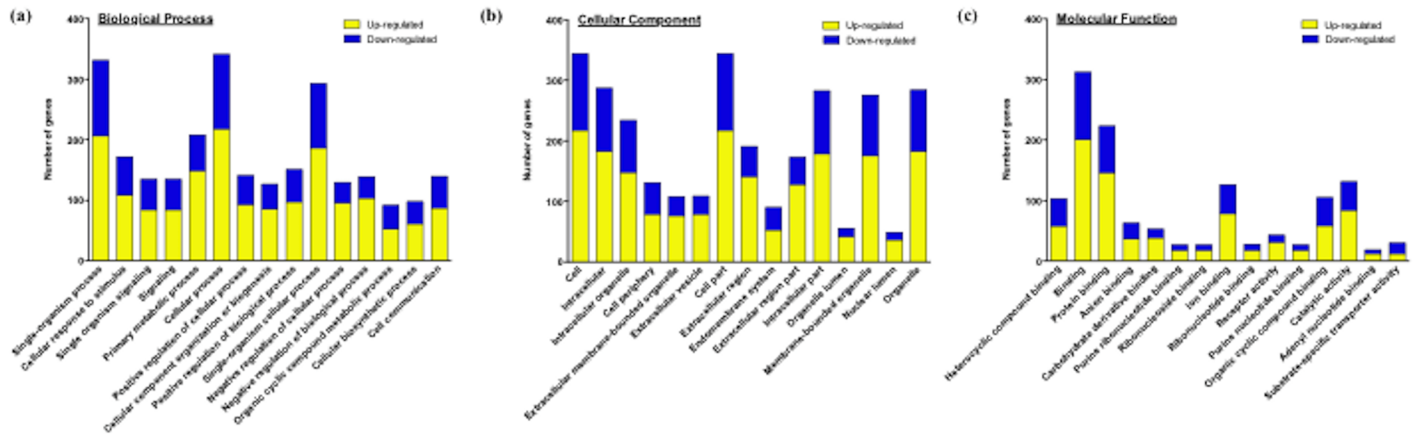


Fig 4. Gene ontology (GO) enrichment analysis of differentially expressed genes in bronchial smooth muscle tissues of the antigen-challenged mice. Total RNA sample of each mouse (4 animals, respectively) was subjected to the microarray analysis, and GO enrichment analysis of differentially expressed genes was performed. Top 15 significant GO terms for biological process (A), cellular component (B) and molecular function (C) are shown (adjusted *p*-value < 0.001 by Bonferroni). Each column represents the number of up- (yellow) and down-regulated (blue) genes in the indicated GO term.

<https://doi.org/10.1371/journal.pone.0202623.g004>

Validation of differentially expressed genes by RT-qPCR

In order to validate the microarray data, differentially expressed mRNA transcripts included in the AA pathway were further analyzed by real-time RT-qPCR (Fig 7). Since the PCR primer design did not allow us to distinguish between *Cyp4a12a* and *Cyp4a12b*, the sum of these transcripts were measured and referred to as *Cyp4a12*. With the exception of *Cyp4a10*, all mRNA transcripts examined showed the concordant up- or down-regulation in BSM tissues of the antigen-challenged mice (Fig 7).

Prostaglandin D₂ level in bronchoalveolar lavage fluids

The results of microarray and RT-qPCR analyses revealed that the expression of phospholipase A₂ (*Pla2g4c*), cyclooxygenase-2 (*Ptgs2*) and prostaglandin D synthase (*Hpgds*) were significantly increased in BSM tissues of the antigen-challenged mice. Immunoblot analysis also revealed an up-regulation of HPGDS protein in BSM tissues of the diseased mice (Fig 8A). The findings also strongly suggest that the AA metabolism is largely shifted towards prostaglandin D₂ (PGD₂) production in BSM tissues of the murine asthma model. To determine the changes in AA metabolism in the airways, lipid mediators in bronchoalveolar lavage (BAL) fluids were measured using LC/MS/MS and ELISA.

In BAL fluids of the mice, a total of 78 lipid species were able to measure by using LC/MS/MS approach. Among them, a total of 27 AA-related metabolites were consistently detected in samples (Fig 9). The level of AA itself in BAL fluids of the antigen-challenged mice (284.5 ± 81.7 pg/mL) was significantly higher than that of control animals (22.2 ± 7.2 pg/mL, *P* < 0.05 by unpaired Student's *t*-test). In the repeatedly antigen-challenged group, most of the AA-related metabolites including PGD₂ were increased (Fig 9B), but the levels of 6-keto-prostaglandin F₁alpha (6-keto-PGF₁alpha; 952.1 ± 44.2 pg/mL in control *versus* 60.2 ± 27.0 pg/mL in challenged mice, *P* < 0.001 by unpaired Student's *t*-test) and 12S-hydroxy-5Z,8E,10E-heptadecatrienoic acid (12-HHT; 6.4 ± 0.9 pg/mL in control *versus* 0.4 ± 0.4 pg/mL in challenged mice, *P* < 0.001 by unpaired Student's *t*-test) were significantly decreased. The levels of PGD₂ in BAL fluids were further determined using an ELISA system. As shown in Fig 8B, the PGD₂ level in BAL fluids of the antigen-challenged mice was significantly higher than that of control animals (*P* < 0.001 by unpaired Student's *t*-test).

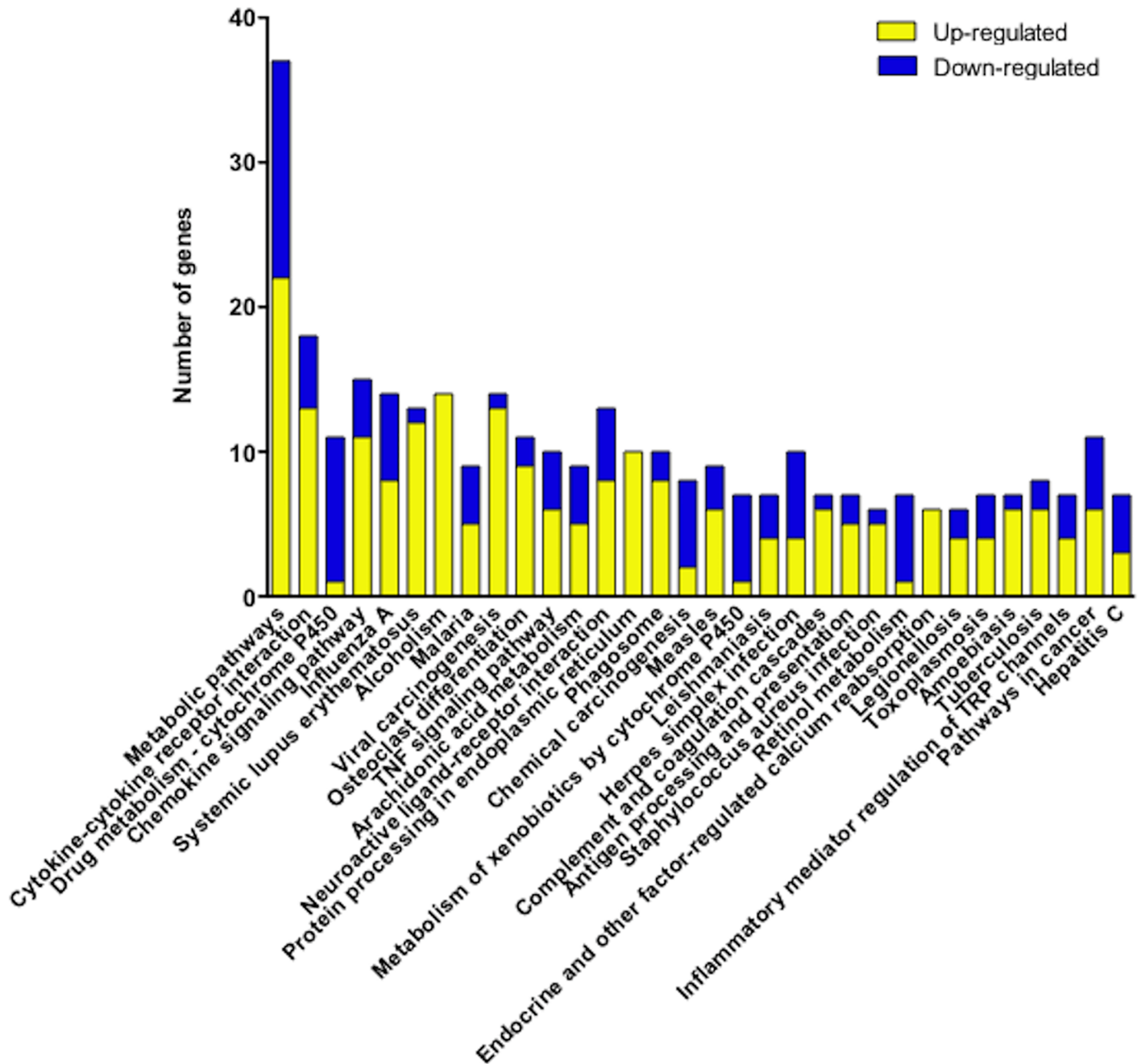


Fig 5. Kyoto Encyclopedia of Genes and Genomes (KEGG) pathway analysis of differentially expressed genes in bronchial smooth muscle tissues of the antigen-challenged mice. Significantly affected pathways are shown (adjusted *P*-value < 0.05 by Bonferroni). Total RNA sample of each mouse (4 animals, respectively) was subjected to the microarray analysis, and KEGG pathway analysis of differentially expressed genes was performed. Each column represents the number of up- (yellow) and down-regulated (blue) genes in the indicated pathway.

<https://doi.org/10.1371/journal.pone.0202623.g005>

Effects of prostaglandin D₂ on BSM function

To determine the role of prostaglandin D₂ (PGD₂) on the AHR, effects of PGD₂ on the isometric tension of smooth muscles were examined in BSM tissues isolated from naive control mice. Application of PGD₂ (10⁻⁹~10⁻⁵ M) had no effect on basal tone of the BSM tissues (data not

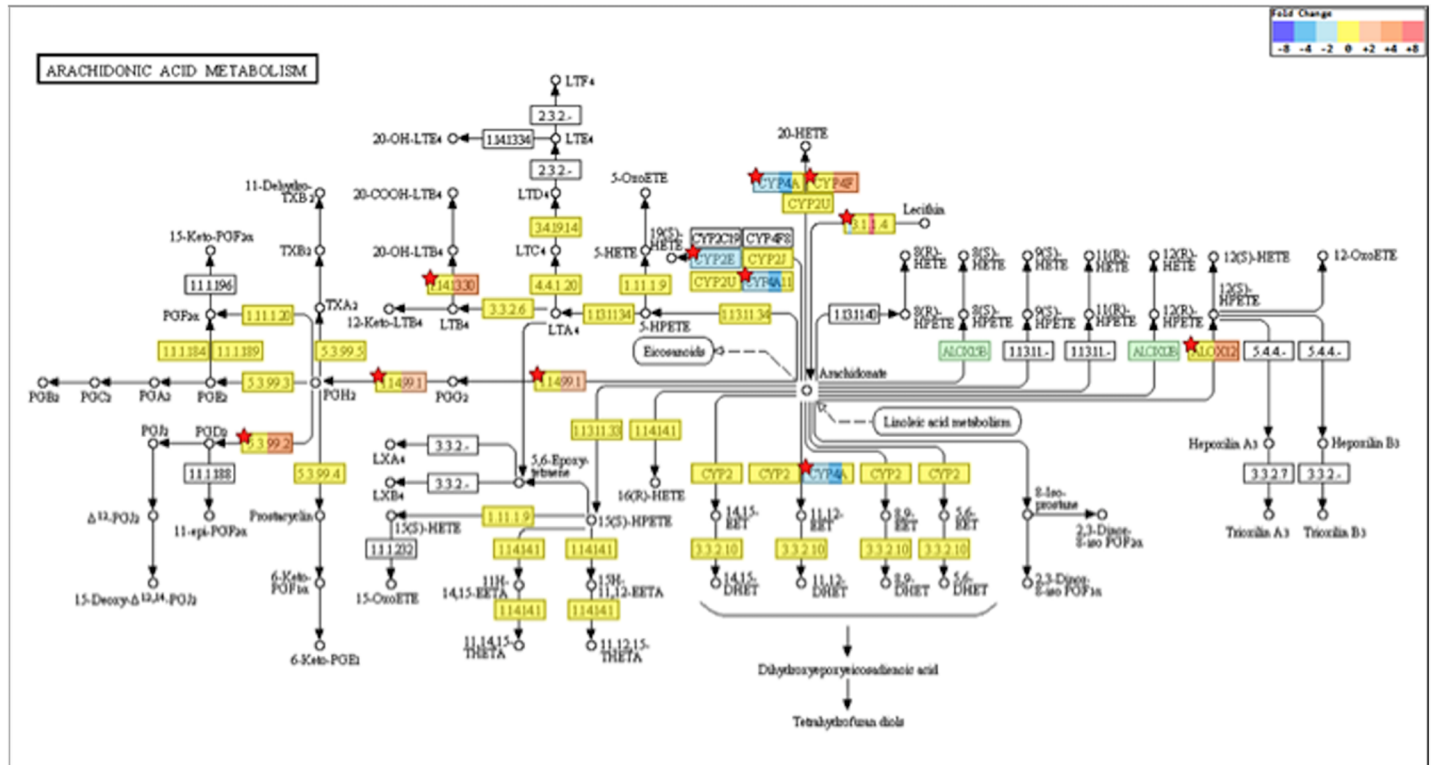


Fig 6. Change in the arachidonic acid metabolism pathway (KEGG map ID: mmu00590) based on the differentially expressed genes in bronchial smooth muscle tissues of the antigen-challenged mice. Total RNA sample of each mouse (4 animals, respectively) was subjected to the microarray analysis, and Kyoto Encyclopedia of Genes and Genomes pathway analysis of differentially expressed genes was performed. Enzymatic reactions are marked by arrows. Fold change values of differentially expressed genes are shown in colors. Different colors in a box for the same module indicate various genes with differing expression. White boxes of pathway map indicate modules that are not relevant to the mouse. Green color boxes of pathway map indicate modules that are not mapped (the gene is in the pathway map but its expression was not shown in the present study). The pathway modules containing differentially expressed genes with statistical significance are marked with red stars.

<https://doi.org/10.1371/journal.pone.0202623.g006>

shown). When the BSM tissues were pre-contracted with 10^{-5} M ACh (about a half-maximal contraction) or 60 mM K^+ (in the presence of 10^{-6} M atropine), cumulatively applied PGD_2 (10^{-9} ~ 10^{-5} M) showed a complicated response. A transient inhibitory effect was observed at the PGD_2 concentration of 10^{-6} M: this was followed by an enhancing effect by the application of 10^{-5} M of PGD_2 (data not shown), indicating that a higher concentration of PGD_2 , at least, could augment the BSM contraction in naive control animals. So in the present study, effects

Table 2. Differentially expressed genes included in the arachidonic acid metabolism pathway (KEGG Map ID: mmu00590) in bronchial smooth muscles of mice with allergic asthma.

| Probe ID | Gene_Symbol | Gene_ID | RefSeq Accession | Fold change | Adjusted P-value |
|---------------|-------------|---------|------------------|-------------|------------------|
| A_52_P17207 | Pla2g4c | 232889 | NM_001168504 | 9.890340 | 0 |
| A_55_P2487484 | Cyp4f18 | 72054 | NM_024444 | 6.538004 | 2.75667E-10 |
| A_51_P471659 | Alox12e | 11685 | NM_145684 | 4.582966 | 1.13732E-06 |
| A_51_P254855 | Ptgs2 | 19225 | NM_011198 | 3.418893 | 0.000107618 |
| A_52_P536796 | Hpgds | 54486 | NM_019455 | 3.251222 | 0.004657938 |
| A_51_P283456 | Cyp2e1 | 13106 | NM_021282 | -2.780193 | 2.87373E-05 |
| A_55_P2092030 | Cyp4a10 | 13117 | NM_010011 | -3.643348 | 2.38762E-08 |
| A_55_P2152607 | Cyp4a12b | 13118 | NM_172306 | -3.908007 | 9.61085E-12 |
| A_55_P2043083 | Cyp4a12a | 277753 | NM_177406 | -4.040550 | 3.26138E-13 |

<https://doi.org/10.1371/journal.pone.0202623.t002>

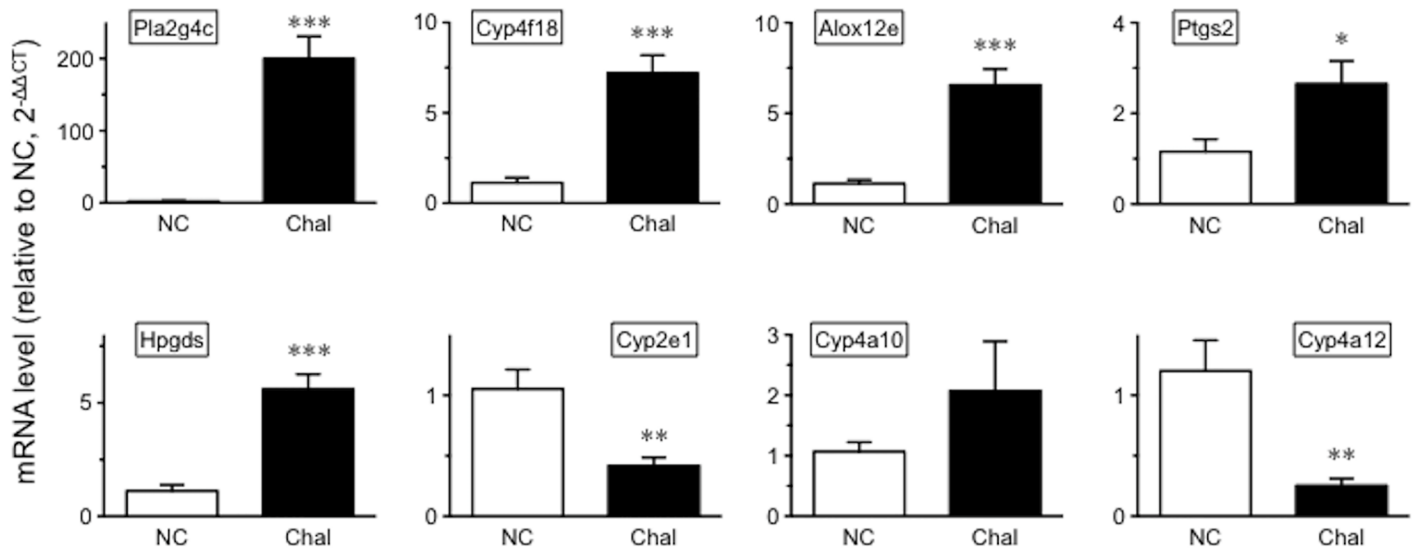


Fig 7. Quantitative RT-PCR validation of differentially expressed genes included in the arachidonic acid metabolism pathway in bronchial smooth muscle tissues of the antigen-challenged mice. Each column represents the mean ± SEM from 6 animals in duplicate, respectively. NC: naive control, and Chal: repeatedly antigen-challenged groups. **P* < 0.05, ***P* < 0.01 and ****P* < 0.001 by unpaired Student's *t*-test.

<https://doi.org/10.1371/journal.pone.0202623.g007>

of pre-treatment with PGD₂ (10⁻⁵ M) on the BSM responsiveness to ACh were determined. As shown in Fig 10A, a 15-min treatment with PGD₂ had no effect on the BSM responsiveness to ACh. However, the ACh concentration-response curve was significantly shifted upward when the BSM tissues were incubated with PGD₂ for 24 hours (Fig 10B).

Discussion

Augmented contractility of airway smooth muscles is one of the causes of the AHR in asthmatics [1–4, 24]. However, the mechanism of the altered properties of airway smooth muscle cells is not fully understood now. In the present study, we focused on BSM tissues of the antigen-challenged mice that have both *in vivo* AHR [20] and hyper-contractility of the isolated BSM tissues (Fig 1). To screen differentially expressed genes of the diseased BSM tissues, a DNA microarray analysis was applied using total RNA extracted from the BSM tissues. Of the 56,605 probe sets represented on the gene chip used, 557 were up-regulated and 213 were down-regulated (see Results section), indicating that gene expression is abundantly changed in the BSM tissues of asthma. The KEGG pathway analysis of the microarray data revealed a significant change in the AA metabolism pathway in BSM tissues of the antigen-challenged mice (Fig 5). In particular, an augmentation of PLA₂ group 4c (*Pla2g4c*)/COX-2 (*Ptgs2*)/PGD₂ synthase 2 (*Hpgds*) cascade was strongly suggested (Fig 6). Expression of these genes in smooth muscle cells of the airways has also been shown by the published gene expression data (GEO accession number GSE45723) [25] and the current study (S2 Fig).

Eicosanoids, including prostaglandins, thromboxanes and leukotrienes, are important signaling molecules that have been implicated in various pathological processes including asthma [26–28]. Their precursor AA is freed from cell membrane phospholipid by the action of PLA₂ family of enzymes. In mice, 20 genes of the PLA₂ family (EC: 3.1.1.4) are listed in the KEGG AA metabolism pathway (Map ID: mmu00590). Among them, a total of 12 genes, *Pla2g2c*, *Pla2g2d*, *Pla2g4a*, *Pla2g5*, *Pla2g4b*, *Pla2g16*, *Pla2g4c*, *Pla2g3*, *Pla2g2e*, *Pla2g6*, *Pla2g12a*, and *Plb1*, were consistently expressed in the BSM tissues by the current microarray analysis. Among the 12 genes expressed, a dramatic increase in *Pla2g4c* (PLA₂ group 4c) was observed

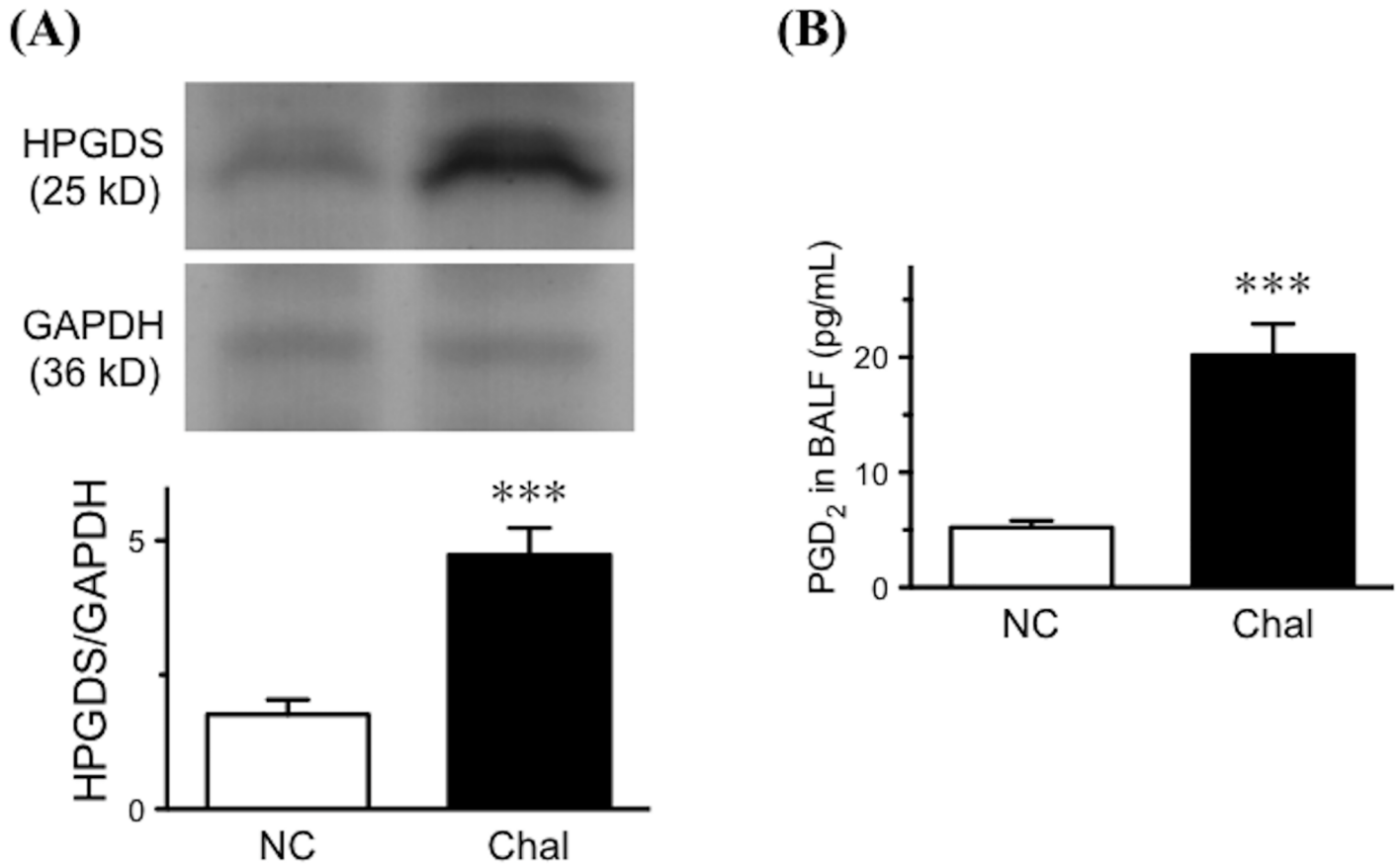


Fig 8. (A) Change in the expression levels of hematopoietic prostaglandin D synthase (HPGDS) protein determined by immunoblottings. (Upper panel) Representative blots for HPGDS and GAPDH. The bands analyzed by a densitometer and normalized by the intensity of corresponding GAPDH band, and the data are summarized in the lower panel. Results are presented as mean ± SEM from 5 animals in duplicate, respectively. ****P* < 0.001 by unpaired Student's *t*-test. **(B) Change in prostaglandin D₂ (PGD₂) level in bronchoalveolar lavage (BAL) fluids of the antigen-challenged mice.** Twenty-four hours after the last antigen challenge, BAL fluids were obtained, and PGD₂ concentrations in BAL fluids were determined by enzyme-linked immunosorbent assay. Results are presented as mean ± SEM from 5 animals in triplicate, respectively. ****P* < 0.001 by unpaired Student's *t*-test.

<https://doi.org/10.1371/journal.pone.0202623.g008>

in BSM tissues of the OA-challenged mice as compared to those of control animals (Table 2 and Fig 7). The results might be consistent with previous report where an increase in the expression of *Pla2g4c* was demonstrated in lungs of a murine asthma model induced by *Aspergillus fumigatus* [29]. It is thus possible that increased expression of *Pla2g4c* is a ubiquitous event in the airways of allergic asthma. PLA₂ group 4c, also named as cytosolic PLA₂gamma (cPLA₂gamma), was first identified by Pickard and colleagues [30], and is a Ca²⁺-independent enzyme on its PLA₂ activity [31, 32]. Cells overexpressing cPLA₂gamma could cause an increase in AA release [31, 33, 34]. Elevated levels of AA in BAL fluids were reported in asthmatics after inhaled antigen challenge [35]. Thus, up-regulation of PLA₂ group 4c might be responsible for the increased AA level in the airways (Fig 9) and the subsequent increase in eicosanoids that are implicated in asthma pathology [26–28].

PGD₂ is an acidic lipid mediator derived from the metabolism of AA by the action of cyclooxygenases, COX-1 (*Ptgs1*) and COX-2 (*Ptgs2*), and downstream PGD₂ synthases, lipocalin-type PGD synthase (*Ptgds*) and hematopoietic PGD synthase (*Hpgds*). Current microarray analyses revealed that these genes were expressed in BSM tissues of the mice. Among them, the mRNA expression levels of *Ptgs2* and *Hpgds* were significantly increased in BSM tissues of the

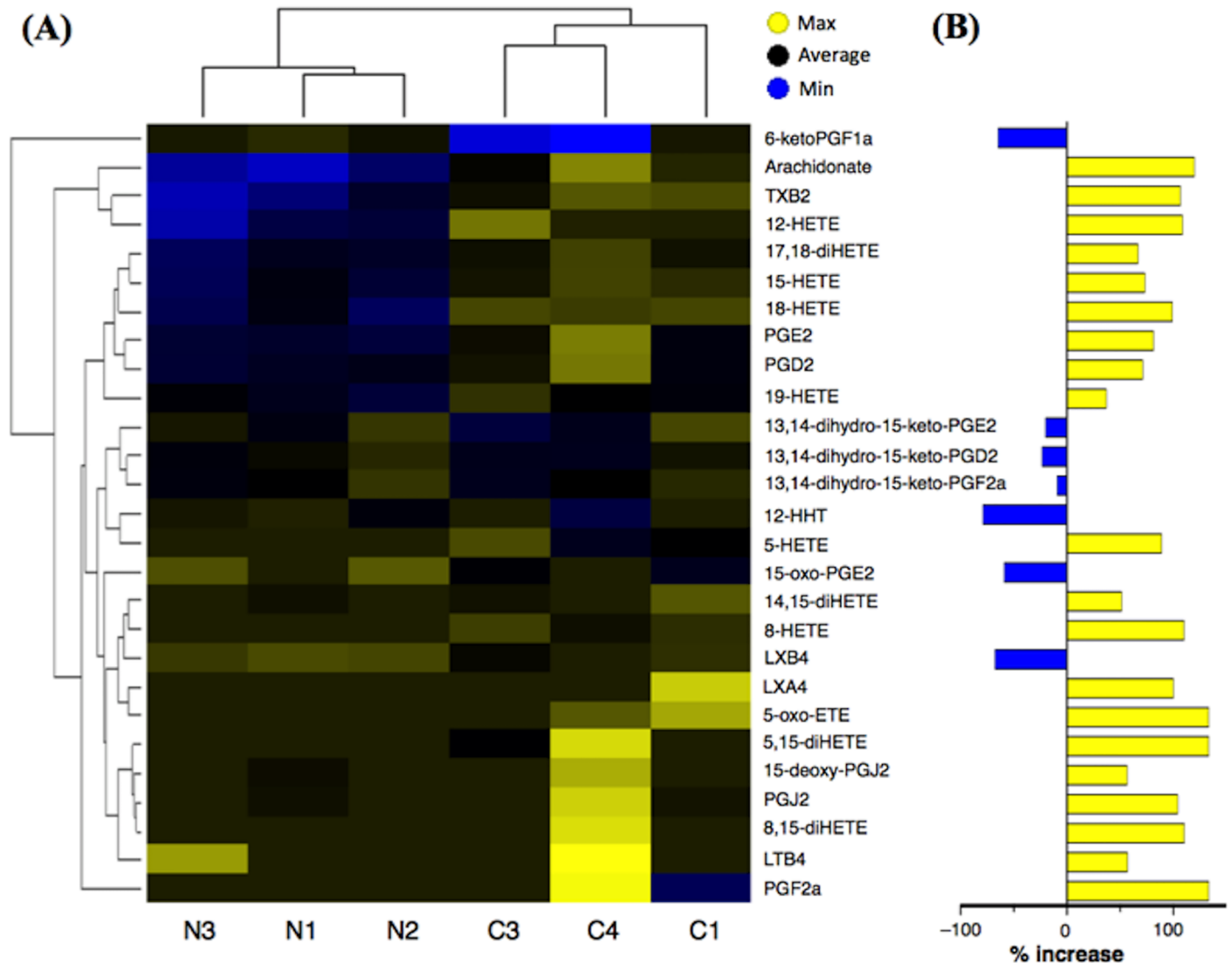


Fig 9. Profiling of changes in arachidonic acid metabolites in bronchoalveolar lavage (BAL) fluids of the antigen-challenged mice. Twenty-four hours after the last antigen challenge, BAL fluids were obtained from respective mice. The BAL fluid of each mouse (3 animals/group) was subjected to the LC/MS/MS analysis as described in METHODS. (A) Hierarchical cluster analysis of arachidonic acid metabolites measured. Each row represents a metabolite and each column represents an individual mouse. N and C represent the normal control and the repeatedly antigen-challenged groups, respectively. Each group contains three different animals. Colors represent fold change in each individual, with yellow indicating increased metabolites and blue indicating decreased metabolites with respect to the average of the normal control animals. (B) Summary of % changes in the metabolite levels in BAL fluids of antigen-challenged mice. Yellow columns indicate % increases and blue columns indicate % decreases of the indicated arachidonic acid metabolites.

<https://doi.org/10.1371/journal.pone.0202623.g009>

OA-challenged animals (Fig 6 and Table 2). Likewise, an increased expression of COX-2 has been demonstrated in lungs of guinea pig asthma model [36] and airway smooth muscles of patients with asthma [37]. Cytokine stimulation could cause an induction of COX-2 in human airway smooth muscle cells [38, 39]. An up-regulation of HPGDS has also been reported in airway structural cells of asthmatics [40]. It is thus possible that the AA metabolism might largely shift towards PGD₂ production in the airways of asthma. Indeed, a significant increase in PGD₂ was also observed in BAL fluids of the OA-challenged mice (Figs 8 and 9).

To determine the role of PGD₂ on smooth muscle function of the airways, the BSMs isolated from naive control mice were treated with PGD₂. Reportedly, PGD₂ has an ability to

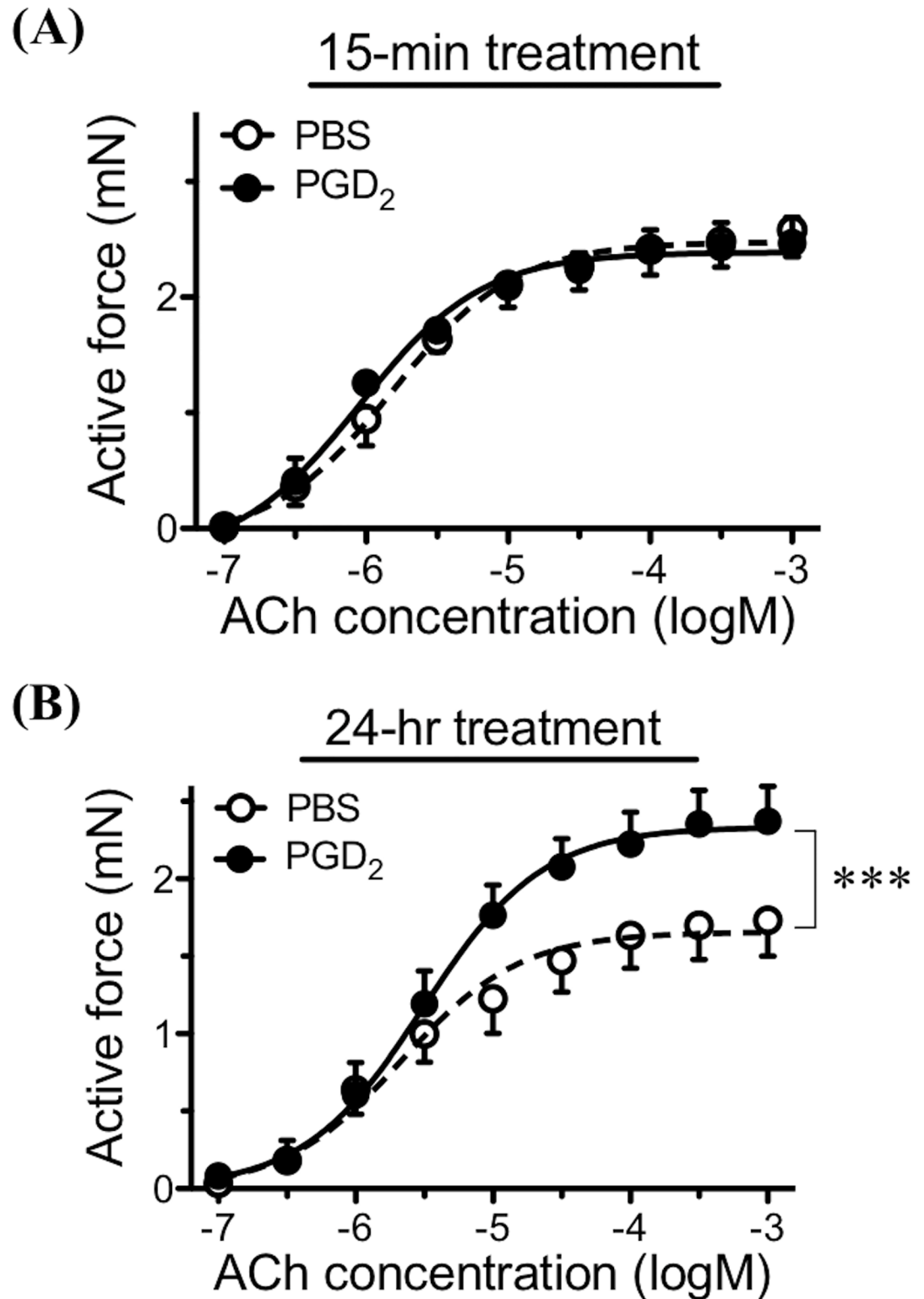


Fig 10. Effect of prostaglandin D₂ (PGD₂) on bronchial smooth muscle (BSM) contractility in naive mice. The BSM tissues isolated from naive BALB/c mice (6 animals) were incubated with PGD₂ (10⁻⁵ M; closed circles) or its vehicle (PBS; open circles) for 15 minutes (A) or 24 hours (B). The BSM responsiveness to cumulatively applied acetylcholine (ACh) was measured as described in METHODS. The ACh concentration-response curve was significantly shifted upward when the BSMs were incubated with PGD₂ for 24 hours (B: ***P < 0.001 by one-way ANOVA with *post hoc* Dunnett).

<https://doi.org/10.1371/journal.pone.0202623.g010>

cause contraction of the isolated airway smooth muscles in guinea pigs [41, 42], rabbits [43] and dogs [44]. The contraction seems to be mediated partly by stimulating cholinergic neurotransmission [41, 44]. However, the current organ bath studies revealed that application of PGD₂ did not affect on baseline tension of the mouse BSMs (see Results), indicating that there is species differences in the effect of PGD₂ on airway smooth muscle function. On the other hand, PGD₂ might be capable of inducing BSM hyper-contractility: PGD₂ augmented the sub-maximal contraction induced by ACh (see Results) and high-K⁺ depolarization (in the presence of 10⁻⁶ M atropine: data not shown). Moreover, the 24-h incubation with PGD₂ caused a BSM hyperresponsiveness to ACh (Fig 10B), as if that was observed at 24 h after the antigen challenge in the asthmatic animals (Fig 1). These findings suggest that the increased PGD₂ level in the airways (Figs 8 and 9) is one of the causes of the antigen-induced BSM hyperresponsiveness.

In the present study, although the BSM contractility was significantly augmented in the antigen-challenged mice (Fig 1), no significant change in the expression levels of genes related to the smooth muscle contraction, such as myosins (*Myh11*, *Myl6*, *Myl9*), actins (*Acta2*, *Actg2*), myosin light chain kinases (MLCKs: *Mylk*, *Mylk2~4*), MLC phosphatases (MLCPs: *Ppp1r12a*, *Ppp1r12b*, *Ppp1r12c*, *Ppp1ca*, *Ppp1cb*, *Ppp1cc*), and caldesmon (*Cald1*), was detected by the current microarray analysis. In this animal model of asthma, an augmented RhoA-mediated Ca²⁺ sensitization of the BSM contraction is a cause of the BSM hyper-contractility [21]. It has also been demonstrated that an inhibition of negative regulation mediated by a microRNA (miRNA), miR-133a-3p, is the main cause of the up-regulation of RhoA protein [18, 45]. Similarly, miRNA regulation of airway smooth muscle function has also been reported [37, 46–50]. It is thus possible that changes in post-transcriptional rather than transcriptional modulations of the gene expression might be largely involved in the alteration of smooth muscle contractility of the diseased airways. PGD₂ might cause such an epigenetic change in airway smooth muscle, resulting in its augmented contractility. Further studies are needed to make clear the exact role of PGD₂ on airway smooth muscle function.

The current LC/MS/MS analysis also revealed a significant decrease in the levels of 6-keto-PGF₁alpha, a stable metabolite of PGI₂, in BAL fluids of the antigen-challenged mice (see Results), indicating that PGI₂ production is decreased in the airways of asthma. PGI₂ is produced from PGH₂, an AA-derived COX metabolite, by the action of PGI₂ synthase (*Ptgis*). Because PGI₂ and its synthetic analogues have been suggested to induce a BSM relaxation [51] and to have an inhibitory effect of asthma including the AHR [51–53], the decreased PGI₂ level in the airways might also be one of the causes of the AHR. Although the mechanism of decrease in PGI₂ level is unclear now, its precursor AA was conversely increased in the diseased airways (see Results). No change in the expression of PGI₂ synthase (*Ptgis*) was observed in the present microarray analysis (fold change: 1.05, adjusted *P*-value: *P* > 0.05). Similarly, the expression of thromboxane A synthase (*Tbxas1*) in the diseased BSM tissues was within control level (fold change: 1.66, adjusted *P*-value: *P* > 0.05). However, the LC/MS/MS approach also revealed a significant decrease in 12-HHT (see Results), whereas a significant increase in TXB₂, a stable metabolite of TXA₂, was observed in BAL fluids of the antigen-challenged mice (15.2 ± 7.6 pg/mL in control versus 99.2 ± 15.6 pg/mL in challenged mice, *P* < 0.01 by unpaired Student's *t*-test). Both 12-HHT and TXA₂ are generated from PGH₂ by the action of *Tbxas1* [54]. It is thus important to note that changes in the levels of lipid mediators in asthma might not be explained simply by changes in the expression of related enzyme genes.

In conclusion, the current study demonstrated that the AA metabolism is largely shifted towards PGD₂ production in BSM tissues of asthma. Increased PGD₂ level in the airways might be one of the causes of airway smooth muscle hyper-contractility, that is a cause of the

AHR in asthmatics. The PLA₂ group 4c/COX-2/PGD₂ synthase 2 cascade might be a potential therapeutic target for AHR in asthma, although some validation studies using human tissues should be required.

Supporting information

S1 Fig. Immunohistochemistry of α -smooth muscle actin (α -SMA) in bronchial smooth muscle (BSM) tissues of mice. The main bronchi were isolated from mice as described in METHODS, and their cryostat sections (4 μ m) were immunostained with anti- α -SMA antibody (1:500 dilution, overnight incubation: Cytoskeleton, Inc.). Typical immunofluorescent images of intact (A) and the mechanically epithelium-denudated BSM tissues (C) and their corresponding light images (B and D, respectively) are shown. e: epithelial layer, bm: basement membrane, and SM: smooth muscle layer. (TIFF)

S2 Fig. Expression of *Pla2g4c*, *Ptgs2* and *Hpgds* in the epithelium-denudated bronchial smooth muscle (BSM) tissues of mice determined by RT-PCR. cDNA samples of the BSMs were amplified using specific primer sets for mouse *Gapdh* (forward primer: 5' -CCTCGTCC CGTAGACAAAATG-3', reverse primer: 5' -TCTCCACTTTGCCACTGCAA-3'), *Pla2g4c* (forward primer: 5' -GGACCGTTGCGTTTTTGTGA-3', reverse primer: 5' -GCAAACCAG CATCCACCAG-3'), *Ptgs2* (forward primer: 5' -CCGTGGGGAATGTATGAGCA-3', reverse primer: 5' -GGGTGGGCTTCAGCAGTAAT-3') and *Hpgds* (forward primer: 5' -TTCCCAT GGGCAGAGAAAAGA-3', reverse primer: 5' -GCCCAGGTTACATAATTGCCT-3'), and detected by 2% agarose gel electrophoresis. Marker: M.W. markers (100 bp ladder). (TIFF)

Acknowledgments

We thank Yusuke Ando, Naomi Takesawa, Misaki Tsuchiyama, Rika Harada, Miku Fujiwara, Yamato Yamane and Yusuke Iwasaki for their technical assistance.

Author Contributions

Conceptualization: Yoshihiko Chiba, Hiroyasu Sakai.

Data curation: Yoshihiko Chiba.

Formal analysis: Yoshihiko Chiba, Wataru Suto.

Funding acquisition: Yoshihiko Chiba.

Investigation: Yoshihiko Chiba, Wataru Suto.

Methodology: Yoshihiko Chiba.

Project administration: Yoshihiko Chiba.

Writing – original draft: Yoshihiko Chiba, Hiroyasu Sakai.

Writing – review & editing: Yoshihiko Chiba.

References

1. Seow CY, Schellenberg RR, Paré PD. Structural and functional changes in the airway smooth muscle of asthmatic subjects. *Am J Respir Crit Care Med* 1998; 158:S179–S186. https://doi.org/10.1164/ajrccm.158.supplement_2.13tac160 PMID: 9817743

2. Martin JG, Duguet A, Eidelman DH. The contribution of airway smooth muscle to airway narrowing and airway hyperresponsiveness in disease. *Eur Respir J* 2000; 16:349–354. PMID: [10968513](#)
3. Ma X, Cheng Z, Kong H, Wang Y, Unruh H, Stephens NL, et al. Changes in biophysical and biochemical properties of single bronchial smooth muscle cells from asthmatic subjects. *Am J Physiol Lung Cell Mol Physiol* 2002; 283:L1181–L1189. <https://doi.org/10.1152/ajplung.00389.2001> PMID: [12388349](#)
4. Björck T, Gustafsson LE, Dahlén SE. Isolated bronchi from asthmatics are hyperresponsive to adenosine, which apparently acts indirectly by liberation of leukotrienes and histamine. *Am Rev Respir Dis* 1992; 145:1087–1091. <https://doi.org/10.1164/ajrccm/145.5.1087> PMID: [1375009](#)
5. Tang DD. Critical role of actin-associated proteins in smooth muscle contraction, cell proliferation, airway hyperresponsiveness and airway remodeling. *Respir Res* 2015; 16:134. <https://doi.org/10.1186/s12931-015-0296-1> PMID: [26517982](#)
6. Chiba Y, Misawa M. The role of RhoA-mediated Ca²⁺ sensitization of bronchial smooth muscle contraction in airway hyperresponsiveness. *J Smooth Muscle Res* 2004; 40:155–167. PMID: [15655303](#)
7. Lambert JA, Song W. Ozone-induced airway hyperresponsiveness: roles of ROCK isoforms. *Am J Physiol Lung Cell Mol Physiol* 2015; 309:L1394–L1397. <https://doi.org/10.1152/ajplung.00353.2015> PMID: [26519207](#)
8. Damera G, Zhao H, Wang M, Smith M, Kirby C, Jester WF, et al. Ozone modulates IL-6 secretion in human airway epithelial and smooth muscle cells. *Am J Physiol Lung Cell Mol Physiol* 2009; 296:L674–L683. <https://doi.org/10.1152/ajplung.90585.2008> PMID: [19201813](#)
9. Vanaudenaerde BM, Wuyts WA, Geudens N, Dupont LJ, Schoofs K, Smeets S, et al. Macrolides inhibit IL17-induced IL8 and 8-isoprostane release from human airway smooth muscle cells. *Am J Transplant* 2007; 7:76–82. <https://doi.org/10.1111/j.1600-6143.2006.01586.x> PMID: [17061983](#)
10. Singh SR, Sutcliffe A, Kaur D, Gupta S, Desai D, Saunders R, et al. CCL2 release by airway smooth muscle is increased in asthma and promotes fibrocyte migration. *Allergy* 2014; 69:1189–1197. <https://doi.org/10.1111/all.12444> PMID: [24931417](#)
11. Clarke DL, Dakshinamurti S, Larsson AK, Ward JE, Yamasaki A. Lipid metabolites as regulators of airway smooth muscle function. *Pulm Pharmacol Ther* 2009; 22:426–435. <https://doi.org/10.1016/j.pupt.2008.12.003> PMID: [19114116](#)
12. Rumzhum NN, Rahman MM, Oliver BG, Ammit AJ. Effect of sphingosine 1-phosphate on cyclo-oxygenase-2 expression, prostaglandin E₂ secretion, and β₂-adrenergic receptor desensitization. *Am J Respir Cell Mol Biol* 2016; 54:128–135. <https://doi.org/10.1165/rcmb.2014-0443OC> PMID: [26098693](#)
13. Rumzhum NN, Patel BS, Prabhala P, Gelissen IC, Oliver BG, Ammit AJ. IL-17A increases TNF-α-induced COX-2 protein stability and augments PGE₂ secretion from airway smooth muscle cells: impact on β₂-adrenergic receptor desensitization. *Allergy* 2016; 71:387–396. <https://doi.org/10.1111/all.12810> PMID: [26606373](#)
14. Calzetta L, Passeri D, Kanabar V, Rogliani P, Page C, Cazzola M, et al. Brain natriuretic peptide protects against hyperresponsiveness of human asthmatic airway smooth muscle via an epithelial cell-dependent mechanism. *Am J Respir Cell Mol Biol* 2014; 50:493–501. <https://doi.org/10.1165/rcmb.2013-0119OC> PMID: [24074453](#)
15. Lortie K, Maheux C, Gendron D, Langlois A, Beaulieu MJ, Marsolais D, et al. CD34 differentially regulates contractile and noncontractile elements of airway reactivity. *Am J Respir Cell Mol Biol* 2018; 58:79–88. <https://doi.org/10.1165/rcmb.2017-0008OC> PMID: [28850257](#)
16. Morin C, Sirois M, Echave V, Gomes MM, Rousseau E. EET displays anti-inflammatory effects in TNF-α stimulated human bronchi: putative role of CPI-17. *Am J Respir Cell Mol Biol* 2008; 38:192–201. <https://doi.org/10.1165/rcmb.2007-0232OC> PMID: [17872494](#)
17. Sutcliffe AM, Clarke DL, Bradbury DA, Corbett LM, Patel JA, Knox AJ. Transcriptional regulation of monocyte chemotactic protein-1 release by endothelin-1 in human airway smooth muscle cells involves NF-κB and AP-1. *Br J Pharmacol* 2009; 157:436–450. <https://doi.org/10.1111/j.1476-5381.2009.00143.x> PMID: [19371341](#)
18. Chiba Y, Tanabe M, Goto K, Sakai H, Misawa M. Down-regulation of miR-133a contributes to up-regulation of RhoA in bronchial smooth muscle cells. *Am J Respir Crit Care Med* 2009; 180:713–719. <https://doi.org/10.1164/rccm.200903-0325OC> PMID: [19644046](#)
19. Jude JA, Tirumurugan KG, Kang BN, Panettieri RA, Walseth TF, Kannan MS. Regulation of CD38 expression in human airway smooth muscle cells: role of class I phosphatidylinositol 3 kinases. *Am J Respir Cell Mol Biol* 2012; 47:427–435. <https://doi.org/10.1165/rcmb.2012-0025OC> PMID: [22556157](#)
20. Kato Y, Manabe T, Tanaka Y, Mochizuki H. Effect of an orally active Th1/Th2 balance modulator, M50367, on IgE production, eosinophilia, and airway hyperresponsiveness in mice. *J Immunol* 1999; 162:7470–7479. PMID: [10358202](#)

21. Chiba Y, Ueno A, Shinozaki K, Takeyama H, Nakazawa S, Sakai H, et al. Involvement of RhoA-mediated Ca²⁺ sensitization in antigen-induced bronchial smooth muscle hyperresponsiveness in mice. *Respir Res* 2005; 6:Art. No. 4.
22. Isobe Y, Arita M, Matsueda S, Iwamoto R, Fujihara T, Nakanishi H, et al. Identification and structure determination of novel anti-inflammatory mediator resolvin E3, 17,18-dihydroxyeicosapentaenoic acid. *J Biol Chem* 2012; 287:10525–10534. <https://doi.org/10.1074/jbc.M112.340612> PMID: 22275352
23. Morita M, Kuba K, Ichikawa A, Nakayama M, Katahira J, Iwamoto R, et al. The lipid mediator protectin D1 inhibits influenza virus replication and improves severe influenza. *Cell* 2013; 153:112–125. <https://doi.org/10.1016/j.cell.2013.02.027> PMID: 23477864
24. Sutcliffe A, Hollins F, Gomez E, Saunders R, Doe C, Cooke M, et al. Airway smooth muscle from individuals with asthma exhibited increased agonist-induced contraction. *Am J Respir Crit Care Med* 2012; 185:267–274.
25. Paez-Cortez J, Krishnan R, Arno A, Aven L, Ram-Mohan S, Patel KR, et al. A new approach for the study of lung smooth muscle phenotypes and its application in a murine model of allergic airway inflammation. *PLoS One* 2013; 8:e74469. <https://doi.org/10.1371/journal.pone.0074469> PMID: 24040256
26. Zaslona Z, Peters-Golden M. Prostanoids in Asthma and COPD: Actions, Dysregulation, and Therapeutic Opportunities. *Chest* 2015; 148:1300–1306.
27. Santus P, Radovanovic D. Prostaglandin D₂ receptor antagonists in early development as potential therapeutic options for asthma. *Expert Opin Investig Drugs* 2016; 25:1083–1092. <https://doi.org/10.1080/13543784.2016.1212838> PMID: 27409410
28. Sanak M. Eicosanoid mediators in the airway inflammation of asthmatic patients: What is new? *Allergy Asthma Immunol Res* 2016; 8:481–490. <https://doi.org/10.4168/air.2016.8.6.481> PMID: 27582398
29. Bickford JS, Newsom KJ, Herlihy JD, Mueller C, Keeler B, Qiu X, et al. Induction of group IVC phospholipase A₂ in allergic asthma: transcriptional regulation by TNF α in bronchoepithelial cells. *Biochem J* 2012; 442:127–137. <https://doi.org/10.1042/BJ20111269> PMID: 22082005
30. Pickard RT, Striffler BA, Kramer RM, Sharp JD. Molecular cloning of two new human paralogs of 85-kDa cytosolic phospholipase A₂. *J Biol Chem* 1999; 274:8823–8831. PMID: 10085124
31. Underwood KW, Song C, Kriz RW, Chang XJ, Knopf JL, Lin LL. A novel calcium-independent phospholipase A₂, cPLA₂- γ , that is prenylated and contains homology to cPLA₂. *J Biol Chem* 1998; 273:21926–21932. PMID: 9705332
32. Lucas KK, Dennis EA. The ABC's of Group IV cytosolic phospholipase A₂. *Biochim Biophys Acta* 2004; 1636:213–218. PMID: 15164769
33. Asai K, Hirabayashi T, Houjou T, Uozumi N, Taguchi R, Shimizu T. Human group IVC phospholipase A₂ (cPLA₂ γ). Roles in the membrane remodeling and activation induced by oxidative stress. *J Biol Chem* 2003; 278:8809–8814. <https://doi.org/10.1074/jbc.M212117200> PMID: 12502717
34. Murakami M, Masuda S, Kudo I. Arachidonate release and prostaglandin production by group IVC phospholipase A₂ (cytosolic phospholipase A₂ γ). *Biochem J* 2003; 372:695–702. <https://doi.org/10.1042/BJ20030061> PMID: 12611587
35. Bowton DL, Seeds MC, Fasano MB, Goldsmith B, Bass DA. Phospholipase A₂ and arachidonate increase in bronchoalveolar lavage fluid after inhaled antigen challenge in asthmatics. *Am J Respir Crit Care Med* 1997; 155:421–425. <https://doi.org/10.1164/ajrccm.155.2.9032172> PMID: 9032172
36. Morin C, Fortin S, Cantin AM, Rousseau É. MAG-EPA resolves lung inflammation in an allergic model of asthma. *Clin Exp Allergy* 2013; 43:1071–1082. <https://doi.org/10.1111/cea.12162> PMID: 23957343
37. Comer BS, Camoretti-Mercado B, Kogut PC, Halayko AJ, Solway J, Gerthoffer WT. Cyclooxygenase-2 and microRNA-155 expression are elevated in asthmatic airway smooth muscle cells. *Am J Respir Cell Mol Biol* 2015; 52:438–447. <https://doi.org/10.1165/rcmb.2014-0129OC> PMID: 25180620
38. Singer CA, Baker KJ, McCaffrey A, AuCoin DP, Dechert MA, Gerthoffer WT. p38 MAPK and NF- κ B mediate COX-2 expression in human airway myocytes. *Am J Physiol Lung Cell Mol Physiol* 2003; 285:L1087–L1098. <https://doi.org/10.1152/ajplung.00409.2002> PMID: 12871860
39. Nie M, Pang L, Inoue H, Knox AJ. Transcriptional regulation of cyclooxygenase 2 by bradykinin and interleukin-1 β in human airway smooth muscle cells: involvement of different promoter elements, transcription factors, and histone h4 acetylation. *Mol Cell Biol* 2003; 23:9233–9244. <https://doi.org/10.1128/MCB.23.24.9233-9244.2003> PMID: 14645533
40. Fajt ML, Gelhaus SL, Freeman B, Uvalle CE, Trudeau JB, Holguin F, et al. Prostaglandin D₂ pathway upregulation: relation to asthma severity, control, and TH2 inflammation. *J Allergy Clin Immunol* 2013; 131:1504–1512. <https://doi.org/10.1016/j.jaci.2013.01.035> PMID: 23506843
41. Omini C, Brunelli G, Daffonchio L, Mapp C, Fabbri L, Berti F. Prostaglandin D₂ (PGD₂) potentiates cholinergic responsiveness in guinea-pig trachea. *J Auton Pharmacol* 1986; 6:181–186. PMID: 3464602

42. Ishimura M, Kataoka S, Suda M, Maeda T, Hiyama Y. Effects of KP-496, a novel dual antagonist for leukotriene D4 and thromboxane A2 receptors, on contractions induced by various agonists in the guinea pig trachea. *Allergol Int* 2006; 55:403–410. <https://doi.org/10.2332/allergolint.55.403> PMID: 17130683
43. Armour CL, Johnson PR, Black JL. Potentiation of contraction of rabbit airway smooth muscle by some cyclooxygenase products. *Prostaglandins* 1988; 35:959–968. PMID: 3187057
44. Tamaoki J, Sekizawa K, Graf PD, Nadel JA. Cholinergic neuromodulation by prostaglandin D₂ in canine airway smooth muscle. *J Appl Physiol* 1987; 63:1396–1400. <https://doi.org/10.1152/jappl.1987.63.4.1396> PMID: 2891674
45. Carè A, Catalucci D, Felicetti F, Bonci D, Addario A, Gallo P, et al. MicroRNA-133 controls cardiac hypertrophy. *Nat Med* 2007; 13:613–618. <https://doi.org/10.1038/nm1582> PMID: 17468766
46. Jude JA, Dileepan M, Subramanian S, Solway J, Panettieri RA Jr, Walseth TF, et al. miR-140-3p regulation of TNF- α -induced CD38 expression in human airway smooth muscle cells. *Am J Physiol Lung Cell Mol Physiol* 2012; 303:L460–L468. <https://doi.org/10.1152/ajplung.00041.2012> PMID: 22773691
47. Dahan D, Ekman M, Larsson-Callerfelt AK, Turczyńska K, Boettger T, Braun T, et al. Induction of angiotensin-converting enzyme after miR-143/145 deletion is critical for impaired smooth muscle contractility. *Am J Physiol Cell Physiol* 2014; 307:C1093–C1101. <https://doi.org/10.1152/ajpcell.00250.2014> PMID: 25273883
48. Sun M, Lu Q. MicroRNA regulation of airway smooth muscle function. *Biol Chem* 2016; 397:507–511. <https://doi.org/10.1515/hsz-2015-0298> PMID: 26812790
49. Sun Q, Liu L, Wang H, Mandal J, Khan P, Hostettler KE, et al. Constitutive high expression of protein arginine methyltransferase 1 in asthmatic airway smooth muscle cells is caused by reduced microRNA-19a expression and leads to enhanced remodeling. *J Allergy Clin Immunol* 2017; 140:510–524. <https://doi.org/10.1016/j.jaci.2016.11.013> PMID: 28081849
50. Cheng Z, Wang X, Dai L, Jia L, Jing X, Liu Y, et al. Suppression of microRNA-384 enhances autophagy of airway smooth muscle cells in asthmatic mouse. *Oncotarget* 2017; 8:67933–67941. <https://doi.org/10.18632/oncotarget.18913> PMID: 28978085
51. Tamaoki J, Chiyotani A, Takeyama K, Yamauchi F, Tagaya E, Konno K. Relaxation and inhibition of contractile response to electrical field stimulation by Beraprost sodium in canine airway smooth muscle. *Prostaglandins* 1993; 45:363–373. PMID: 8388118
52. Zhou W, Zhang J, Goleniewska K, Dulek DE, Toki S, Newcomb DC, et al. Prostaglandin I₂ suppresses proinflammatory chemokine expression, CD4 T cell activation, and STAT6-independent allergic lung inflammation. *J Immunol* 2016; 197:1577–1586. <https://doi.org/10.4049/jimmunol.1501063> PMID: 27456482
53. Yamabayashi C, Koya T, Kagamu H, Kawakami H, Kimura Y, Furukawa T, et al. A novel prostacyclin agonist protects against airway hyperresponsiveness and remodeling in mice. *Am J Respir Cell Mol Biol* 2012; 47:170–177. <https://doi.org/10.1165/rcmb.2011-0350OC> PMID: 22403804
54. Smith WL, Urade Y, Jakobsson PJ. Enzymes of the cyclooxygenase pathways of prostanoid biosynthesis. *Chem Rev* 2011; 111:5821–5865. <https://doi.org/10.1021/cr2002992> PMID: 21942677